The Astrophysical Journal, 666:609–625, 2007 September 1

POLYCHROMATIC COMPENSATION OF PROPAGATED ABERRATIONS FOR HIGH-CONTRAST IMAGING

Laurent Pueyo and N. Jeremy Kasdin
Department of Mechanical and Aerospace Engineering, Princeton University, Princeton, NJ 08544;
lpueyo@princeton.edu, jkasdin@princeton.edu
Received 2007 February 1; accepted 2007 March 29

ABSTRACT

We describe the influence of Fresnel propagation in apodized-pupil coronagraphs and introduce a methodology to compensate for propagated wavefront aberrations. We start from the Fresnel integral and derive an analytical closed form for the propagated field at an arbitrary distance from a pupil. In a second part, we show that the propagation of the coronagraphic term can be neglected with sufficiently oversized optics. Then we derive a λ-Fourier expansion of the aberration at an arbitrary plane in the optical train of a telescope. Finally, we present a series of wavefront actuators, based on multiple deformable mirrors, that possess adequate chromatic behavior to correct for the dominant terms of this expansion.

Subject headings: instrumentation: adaptive optics — instrumentation: high angular resolution

Online material: color figures

1. INTRODUCTION

Recent work in coronagraphic design and adaptive optics has enabled considerable progress toward a feasible visible-light exoplanet observatory. In particular, apodized-pupil coronagraphs have been intensively studied; while Aime et al. (2002) highlighted the existence of analytical optimal apodizations, Spergel & Kasdin (2001) and, later on, Kasdin et al. (2003) devised a simple method to generate these apodizers using shaped pupils. In the meantime, the feasibility of an experimental dark hole featuring a depth of 10 orders of magnitude has been proved (Trauger & Traub 2007). This wavefront controller is designed to optimally suppress off-axis starlight for a specific wavelength, and under a broadband illumination the magnitude of the residual halo is an increasing function of bandwidth. This effect is due to wavelength-independent reflectivity errors in the optics, to the nonlinear behavior of phase errors, and to Fresnel effects along the optical path. While Noecker et al. (2003) and Give'on et al. (2003) have presented solutions to monochromatically compensate for the first two phenomena, the third has not received much attention. In particular, for slow optics the nature of an aberration, phase or amplitude, changes as an effect of transverse propagation. Indeed, for a space-based coronagraph, Shaklan & Green (2006) showed that propagation effects are the source of phase-induced amplitude errors that cannot be corrected polychromatically by using only a single deformable mirror (DM), thus creating severe surface and reflectivity requirements for a broadband instrument.

The purpose of this paper is to introduce a formalism to treat the wavelength dependence of aberrations that will allow creation of a broadband null by means of several DMs adequately positioned, as suggested by Shaklan & Green (2006) in their initial paper. In classical adaptive optics, the telescope is modeled as a pupil propagating according to ray optics, the aberrations are suppressed using a DM in this pupil plane, and the final image is created by a lens taking the Fourier transform of the flat wavefront. In this communication, we account for the Fresnel propagation between the pupil and the DM, our goal being to develop an understanding of both the phase and amplitude mixing and the wavelength dependence of the aberration at the location of the DM. Then we will be able to develop a multiwavelength estimation scheme in order to create a polychromatic starlight null in the image plane.

2. FRESNEL PROPAGATION OF HARMONIC ABERRATIONS

In a typical imaging system, diffraction analysis considers only the Fraunhofer transformation due to the imaging element, resulting in the usual point-spread function (PSF) at the image plane. However, a careful Fresnel analysis of the electric field's propagation along the optical axis between pupils reveals distortions in the wavefront beyond simple ray optics. These distortions can have a significant impact on the final image. These effects are usually mitigated by oversizing the imaging elements. That is, when the imaging optics, of diameter L, are large compared with the pupil, of diameter D, and when the propagation distance z is short, the effects of such propagation are considered negligible. A common quantifier of the range of validity of this ray-optics approximation is the Fresnel number, $F = D^2/\lambda z$. If F is very large, then it is legitimate to assume that the pupil propagates according to ray optics. The main purpose of this paper is to discard this approximation in the context of high-contrast imaging, in order to develop a more accurate model of coronagraphic adaptive optics (AO). Our approach relies on an analytical derivation of the Fresnel diffraction, presented in this section. Assuming the geometry of Figure 1, we derive the field distribution at a distance z downstream of the pupil plane P_0, with arbitrary apodization $A(x, y)$, to plane P_z. This will provide the needed information to predict the effect of a DM at plane P_z and allow us to calculate the final PSF due to an imaging element after the DM.

2.1. *Propagation Followed by an Imaging Element*

We begin by examining the Fresnel transformation of an arbitrary field followed by a perfect imaging lens.

Theorem 1. *Consider an arbitrary complex electric field, $E_0(x, y)$, at plane P_0. Suppose this field is propagated to plane P_z, at a distance z from P_0, via a Fresnel integration,*

$$E_z(u, v) = \frac{e^{ikz}}{i\lambda z} \iint E_0(x, y) e^{i\pi[(x-u)^2+(y-v)^2]/\lambda z}\, dx\, dy. \tag{1}$$

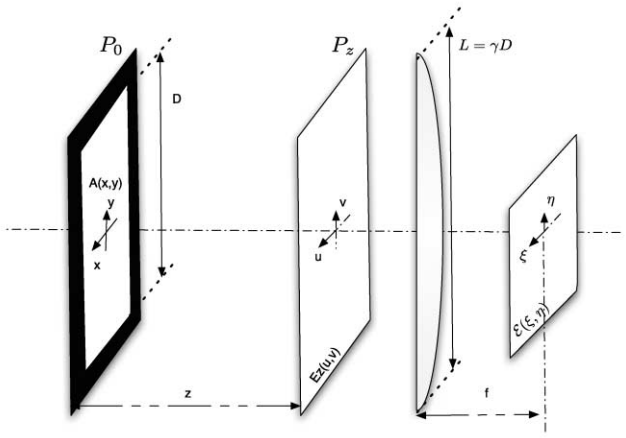

FIG. 1.—Coordinate systems for Fresnel diffraction. Any design that involves Fresnel effects can be reduced to this scheme by a change of variables. The plane P_0 is the pupil plane of the telescope. The distribution $E_0(x, y)$ is then propagated over a distance z to the plane P_z, where the wavefront actuator is located. The field after the actuator is then Fourier-transformed to yield the image $I(\xi, \eta)$.

This propagation is immediately followed by an infinitely large lens, forming an image a distance f away. Then the intensity at the image plane, $I(\xi, \eta)$, is exactly the modulus squared of the Fourier transform of E_0.

Proof. The Fresnel transformation in equation (1) is a convolution between the complex electric field at P_0 and a Gaussian kernel. Its Fourier conjugate can thus be written, where carets represent the Fourier transform,

$$\hat{E}_z(\sigma, \tau) = e^{ikz}\hat{E}_0(\sigma, \tau)e^{-i\pi\lambda z(\sigma^2+\tau^2)} \tag{2}$$

(Goodman 1968). Since the infinite lens produces a Fraunhofer integral, its action is to take the Fourier transform of the field E_z. The intensity distribution in the image plane is therefore given by

$$I(\xi, \eta) = |\hat{E}_z|^2 = |\hat{E}_0|^2. \tag{3}$$

□

In this paper we are mainly concerned with propagations between an entrance pupil and a deformable mirror and among multiple DMs to study the consequences of Fresnel distortions on wavefront control. An important consequence of Theorem 1 is that the location of the final, imaging lens is unimportant. As long as the lens (or mirror) is adequately oversized, we can treat it as lying at the DM's location and compute the final image-plane intensity as a simple Fourier transform of the field leaving the last DM. This result can be extended to the case of multiple propagations, when the beam is reflected by several fold mirrors or goes through an intermediate focus.

COROLLARY 1. *Consider an arbitrary complex electric field, $E_0(x, y)$, at plane P_0. Suppose this field is propagated to planes $P_{z_1,z_2,\ldots,z_p}$ via a number p of Fresnel propagations of distances $z_1, \ldots, z_p$. Assuming that all the optics are aberration-free and infinitely large, then the intensity at the image plane, $I(\xi, \eta)$, is exactly the modulus squared of the Fourier transform of E_0.*

Proof. Since the optics are infinite and the p optics do not add an extra aberration, then the field distribution before the final imaging element can be written as

$$E_{z_1+\cdots+z_p}(u, v) = e^{ik\sum_{j=1}^{p} z_j}\left(\bigotimes_{j=1}^{p} e^{i\pi(x^2+y^2)/\lambda z_j}\right) * E_0(x, y), \tag{4}$$

where the circled cross stands for a multiple convolution. In the Fourier domain, this distribution can be written as

$$\hat{E}_{z_1+\cdots+z_p}(\sigma, \tau) = e^{ik\sum_{j=1}^{p} z_j}e^{-i\pi\lambda(\sigma^2+\tau^2)\sum_{j=1}^{p} z_j}\hat{E}_0(\sigma, \tau). \tag{5}$$

As shown above, the propagation consists only of a phase term in the Fourier domain, meaning that it does not affect the intensity distribution in the image plane:

$$I_{z_1+\cdots+z_p} = |\hat{E}_0|^2. \tag{6}$$

□

We are also mainly interested in apodized systems, where the entrance field E_0 is given by a real amplitude function, $A(x, y)$, times a constant, uniform wavefront. We use the notation $\mathcal{F}_z\mathcal{A}$ to represent the Fresnel transform of the apodization,

$$\mathcal{F}_z\mathcal{A}(u, v) = \frac{e^{ikz}}{i\lambda z}\iint A(x, y)e^{i\pi[(x-u)^2+(y-v)^2]/\lambda z}\,dx\,dy, \tag{7}$$

the Fourier transform of which is then given by

$$\widehat{\mathcal{F}_z\mathcal{A}}(\sigma,\tau) = e^{ikz}\hat{A}(\sigma,\tau)e^{-i\pi\lambda z(\sigma^2+\tau^2)}. \tag{8}$$

Theorem 1 then leads to the identity

$$I(\xi,\eta) = \left|\widehat{\mathcal{F}_z\mathcal{A}}\left(\frac{\xi D}{\lambda f},\frac{\eta D}{\lambda f}\right)\right|^2 = \left|\hat{A}\left(\frac{\xi D}{\lambda f},\frac{\eta D}{\lambda f}\right)\right|^2. \tag{9}$$

Consequently, in the case of infinite optics it is not necessary to carry out a full treatment of the Fresnel integral if one seeks to predict the intensity distribution at the final focal plane of a telescope.

2.2. *Propagation between Conjugate Planes*

There exists another remarkable plane in the optical train of the telescope, called the conjugate of the pupil, where the Fresnel integral simplifies dramatically. Consider the same pupil distribution $E_0(x, y)$ followed by a lens located at a distance z from the pupil. Then geometric optics predicts that an image of the pupil will form at a distance z' from the lens such that $1/f = 1/z + 1/z'$, where f is the focal length of the lens. A full analytical treatment of the Fresnel integral shows that the field distribution $E_{z+z'}(u, v)$ at a distance z' from the lens and the initial distribution $E_0(x, y)$ are related as follows:

$$E_{z+z'}(u,v) = -\frac{z'}{z}e^{i\pi(z'/z)(u^2+v^2)/\lambda f}E_0\left(-\frac{z'}{z}u,-\frac{z'}{z}v\right). \tag{10}$$

The intensity distribution at this plane is a scaled version of the original incident intensity. For any plane other than the image and the conjugate planes, the full Fresnel integral must be solved in order to predict the field distribution.

2.3. *Finite Entrance Pupil and Aberrations*

In this section, we examine the Fresnel propagation of an explicitly aberrated wavefront. To begin, we simplify by considering only a phase aberration, $\phi(x, y)$, on the input field at plane P_a. The field distribution, $E_0(x, y)$, is then given by

$$E_0(x,y) = A(x,y)e^{i\phi(x,y)} \simeq A(x,y)[1 + i\phi(x,y)], \tag{11}$$

where we have assumed a small phase aberration, $\phi \ll 1$. Under this approximation, a phase error becomes an imaginary disturbance of the field in the pupil plane. Likewise, when a DM is inserted in the pupil plane, its first-order effect is a modification of the imaginary part of the field. The more general case of an arbitrarily large phase distortion along with amplitude variations will be treated below.

To derive the propagation of the aberrated pupil distribution in equation (11), we separate the problem into the calculation of two different integrals: the propagation of the aberration, which will be fully derived analytically, and the propagation of the finite apodization function, which is represented by equation (7):

$$\begin{aligned} E_z(u,v) &= \frac{e^{ikz}}{i\lambda z}\iint A(x,y)[1 + i\phi(x,y)]e^{i\pi[(x-u)^2+(y-v)^2]/\lambda z}\,dx\,dy \\ &= \mathcal{F}_z\mathcal{A}(u,v) + \frac{e^{ikz}}{\lambda z}e^{i\pi(u^2+v^2)/\lambda z}\iint A(x,y)\phi(x,y)e^{i\pi(x^2+y^2)/\lambda z}e^{i2\pi(xu+yv)/\lambda z}\,dx\,dy, \end{aligned} \tag{12}$$

where we have multiplied out the exponential. One can now recognize that the second Fresnel integral is the Fourier transform of the product of two functions. It can thus instead be expressed as a convolution of two Fourier integrals, evaluated at $(u/\lambda z, v/\lambda z)$:

$$E_z(u,v) = \mathcal{F}_z\mathcal{A}(u,v) + \frac{e^{ikz}}{\lambda z}e^{i\pi(u^2+v^2)/\lambda z}\{\mathrm{FT}\,[A(x,y)] * \mathrm{FT}\,[\phi(x,y)e^{i\pi(x^2+y^2)/\lambda z}]\}\Big|_{(u/\lambda z,\,v/\lambda z)}. \tag{13}$$

We have thus separated the problem into the convolution of two Fourier integrals. The first one carries information about the apodization and the finiteness of the entrance aperture, $A(x, y)$, while the second integral corresponds to the propagation of the aberration to the second plane, $E_z(u, v)$.

In order to carry out the second Fourier transform analytically, we expand $\phi(x, y)$ in a harmonic series. As mentioned above, we only consider the first-order expansion of a phase error for the present derivation. Since any pupil-plane function can be extended to a D-periodic function and thus decomposed into a Fourier series, our final result will be easily generalizable to amplitude or higher orders of the phase expansion. We thus express the phase error as

$$\phi(x,y) = \sum_n\sum_m \frac{2\pi b_{m,n}\lambda_0}{\lambda}e^{i2\pi(nx+my)/D} = \sum_n\sum_m \phi_{m,n}(x,y), \tag{14}$$

where the $b_{m,n}$ are small and dimensionless and λ_0 is the central wavelength in the spectral band where the observations occur. Linearity allows us to separately examine the propagation of each of the terms, which we call $E_z^{m,n}(u, v)$. To find this, we substitute

a single term from the expansion in equation (14) into equation (13) and write the convolution using the independent variables σ and τ,

$$E_z^{m,n}(u,v) = \frac{e^{ikz}}{\lambda z} e^{i\pi(u^2+v^2)/\lambda z} \iint \hat{A}(\sigma,\tau)\mathrm{FT}\left[\phi(x,y)_{m,n} e^{i\pi(x^2+y^2)/\lambda z}\right]\}\Big|_{(u/\lambda z-\sigma, v/\lambda z-\tau)} d\sigma\, d\tau,$$
$$= \frac{e^{ikz}}{\lambda z}\frac{2\pi b_{m,n}\lambda_0}{\lambda} \iint \hat{A}(\sigma,\tau) e^{-i\pi\lambda z(\sigma^2+\tau^2)} e^{i2\pi(\sigma u+\tau v)} \iint e^{i2\pi(mx+ny)/D} e^{i\pi[(x-u+\lambda z\sigma)^2+(y-v+\lambda z\tau)^2]/\lambda z}\, dx\, dy\, d\sigma\, d\tau, \quad (15)$$

where we have collected all the (x, y)-dependent terms in the second integral and completed the square of the exponential in that same integrand. The integrand of the first integral is given exactly in equation (8), which we recognize as the propagation of the apodization function. Computing the propagation of a harmonic aberration has thus been reduced to the computation of the following integral for each harmonic term:

$$\frac{1}{\lambda z}\iint e^{i2\pi(mx+ny)/D} e^{i\pi[(x-u-\lambda z\sigma)^2+(y-v-\lambda z\tau)^2]/\lambda z}\, dx\, dy = ie^{i2\pi[n(u+\lambda z\sigma)+m(v+\lambda z\tau)]/D} e^{-i\pi\lambda z(n^2+m^2)/D^2}. \quad (16)$$

$E_z^{m,n}(u, v)$ then simplifies to

$$E_z^{m,n}(u,v) = ie^{ikz}\frac{2\pi b_{m,n}\lambda_0}{\lambda} e^{i2\pi(nu+mv)/D} e^{-i\pi\lambda z(n^2+m^2)/D^2} \iint \hat{A}(\sigma,\tau) e^{-i\pi\lambda z(\sigma^2+\tau^2)} e^{i2\pi(n\lambda z\sigma+m\lambda z\tau)/D} e^{i2\pi(u\sigma+v\tau)}\, d\sigma\, d\tau. \quad (17)$$

Equation (17) is the inverse Fourier transform of $\widehat{\mathcal{F}_z\mathcal{A}}(\sigma, \tau)$ multiplied by a harmonic term; thus, using the Fourier shift theorem,

$$E_z^{m,n}(u,v) = ie^{i2\pi(nu+mv)/D} e^{i\pi\lambda z(n^2+m^2)/D^2} \mathcal{F}_z\mathcal{A}\left(u-\frac{n\lambda z}{D}, v-\frac{m\lambda z}{D}\right), \quad (18)$$

which yields, once all the terms of the initial harmonic series have been added, the final expansion that is expressed in the following lemma:

Lemma 1. *Consider the propagation of the pupil of a telescope whose transmittivity function is given by $A(x, y)$ and that is subject to a phase aberration $\phi(x, y)$. Assume moreover that the phase errors are small enough so that a first-order approximation holds and that they can be expanded in a Fourier series $\phi(x, y) = \sum_{m,n}(2\pi b_{m,n}\lambda_0/\lambda)e^{i2\pi(mx+ny)/D}$. Then the propagated field can be written as a function of the Fresnel transform of the apodization $\mathcal{F}_z\mathcal{A}(u, v)$,*

$$E_z(u,v) = \mathcal{F}_z\mathcal{A}(u,v) + i\sum_m\sum_n \frac{2\pi b_{m,n}\lambda_0}{\lambda} e^{i2\pi(nu+mv)/D} e^{-i\pi\lambda z(n^2+m^2)/D^2} \mathcal{F}_z\mathcal{A}\left(u-\frac{n\lambda z}{D}, v-\frac{m\lambda z}{D}\right). \quad (19)$$

2.4. *Interpretation of This Result*

This expansion is an analytical closed form for the propagation of an aberrated field. It is composed of the Fresnel-propagated apodization function, $\mathcal{F}_z\mathcal{A}(u, v)$, and an additional sum due to the propagation of the aberration. In this sum, each term consists of a harmonic aberration windowed by a shifted $\mathcal{F}_z\mathcal{A}(u, v)$ and multiplied by the angular spectrum factor. First note that the propagation of the initial amplitude distribution, and of the sharp edges, which cause many numerical problems in particular, is all contained in $\mathcal{F}_z\mathcal{A}$. The location of this propagated apodization is shifted, and the shift depends on the spatial frequency. The exponential angular spectrum factor that is present for each spatial frequency is identical to the one for an infinite aperture, as presented by Goodman (1968).

The propagation of sharp edges contained in $\mathcal{F}_z\mathcal{A}(u, v)$ is the central problem of numerical calculations associated with Fresnel propagation. We show in the next section that the problem can be further reduced to the propagation of open square apertures. The shifted pupil function can be explained by considering that each harmonic component behaves as a diffraction grating and shifts $\mathcal{F}_z\mathcal{A}(u, v)$ to the location of the first diffraction order. For reasonably large optics, $\lambda z/D$ is a very small number, and thus this shift is extremely small compared with the size of the pupil.

Of more interest is the angular spectrum factor, since it is responsible for a real-imaginary coupling of the Fourier coefficients that is often called phase-induced amplitude error. To illustrate this, consider the two terms associated with $b_{m,n}$ and $b_{-m,-n} = b^*_{m,n}$ in equation (19),

$$\frac{i2\pi b_{m,n}\lambda_0}{\lambda} e^{i2\pi(nu+mv)/D} e^{i\pi\lambda z(n^2+m^2)/D^2} \mathcal{F}_z\mathcal{A}\left(u-\frac{n\lambda z}{D}, v-\frac{m\lambda z}{D}\right)$$
$$+\frac{i2\pi b^*_{m,n}\lambda_0}{\lambda} e^{i2\pi-(nu+mv)/D} e^{i\pi\lambda z(n^2+m^2)/D^2} \mathcal{F}_z\mathcal{A}\left(u+\frac{n\lambda z}{D}, v+\frac{m\lambda z}{D}\right)$$
$$\approx \frac{i2\pi\lambda_0}{\lambda} e^{i\pi\lambda z(n^2+m^2)/D^2} \mathcal{F}_z\mathcal{A}(u,v)(b_{m,n}e^{i2\pi(nu+mv)/D} + b^*_{m,n}e^{-i2\pi(nu+mv)/D})$$
$$\approx \frac{i2\pi\lambda_0}{\lambda} \mathcal{F}_z\mathcal{A}(u,v) e^{i\pi\lambda z(n^2+m^2)/D^2}\,\mathrm{Re}\,(b_{m,n}e^{i2\pi(nu+mv)/D}). \quad (20)$$

Thus, what was a purely imaginary aberration in plane P_0 became both real and imaginary at plane P_z. Consequently, a device purely correcting for imaginary disturbances in plane P_z, such as a DM, would not be able to compensate for the real part of the propagated aberration. Moreover, the nonlinear wavelength dependence of this coupling makes the polychromatic compensation of these effects a challenging problem. For low-to-mid spatial frequencies, Shaklan & Green (2006) simplified this problem by carrying out a first-order expansion of the angular spectrum factor,

$$i\frac{2\pi\lambda_0}{\lambda}\mathcal{F}_z\mathcal{A}(u,v)e^{i\pi\lambda z(n^2+m^2)/D^2}\,\mathrm{Re}\,(b_{m,n}e^{i2\pi(nu+mv)/D}) \simeq \mathcal{F}_z\mathcal{A}(u,v)\,\mathrm{Re}\,(b_{m,n}e^{i2\pi(nu+mv)/D})\left[i\frac{2\pi\lambda_0}{\lambda}+\frac{2\pi^2 z(n^2+m^2)\lambda_0}{D^2}\right], \quad (21)$$

which shows that to the first order in $\pi z(n^2 + m^2)\lambda_0/D^2$, phase-induced amplitude errors are wavelength independent.

2.5. *Harmonic Expansion of the Apodization*

Previously we derived the analytical propagation of a harmonic aberration transmitted by an arbitrary apodizer in terms of the Fresnel transform of the apodizer, $\mathcal{F}_z\mathcal{A}(u, v)$; our final step is to derive an analytical expression for this distribution in terms of special functions. In the calculations leading to Lemma 1, the assumption of phase-only errors was made for purposes of illustration; the exact same approach could be carried out using amplitude errors.

This can be generalized to the following theorem:

THEOREM 2. *Consider the propagation of the pupil of a telescope whose complex transmittivity function is given by $A(x, y)h(x, y)$, where $A(x, y)$ is a real apodization function and $h(x, y)$ is a complex disturbance at the pupil plane. Assume moreover that $h(x, y)$ is inscribed within a square of size D so that it can be decomposed in a complex Fourier series: $h(x, y) = \sum_{m,n} h_{m,n}e^{i2\pi(mx+ny)/D}$. Then the propagated field can be written as a function of the Fresnel transform of the apodization $\mathcal{F}_z\mathcal{A}(u, v)$,*

$$E_z(u,v) = \mathcal{F}_z\mathcal{A}(u,v) + \sum_m\sum_n h_{m,n}e^{i2\pi(nu+mv)/D}e^{-i\pi\lambda z(n^2+m^2)/D^2}\mathcal{F}_z\mathcal{A}\left(u-\frac{n\lambda z}{D}, v-\frac{m\lambda z}{D}\right). \quad (22)$$

We can use Theorem 2 to further simplify the Fresnel propagation of the apodization $A(x, y)$. We decompose $A(x, y)$ into an amplitude Fourier series multiplied by a top-hat function. To simplify, we consider the case of an apodization inscribed in a square aperture,

$$A(x,y) = \pi_D(x,y)\sum_{m,n} a^0_{m,n}e^{i2\pi(nx+my)/D}, \quad (23)$$

where the coefficient $a^0_{0,0}$ corresponds to the on-axis transmittivity of the apodization. Then the pupil can be propagated over a distance z by using equation (19). The information about the shape of the apodization is contained in the $a^0_{m,n}$, and the new transmittivity function is an open aperture of size D: $\pi_D(x, y)$. The propagated field is thus

$$\mathcal{F}_z\mathcal{A}(u,v) = \sum_m\sum_n a^0_{m,n}e^{i2\pi(nu+mv)/D}e^{-i\pi\lambda z(n^2+m^2)/D^2}\mathcal{F}_z\Pi\left(u-\frac{n\lambda z}{D}, v-\frac{m\lambda z}{D}\right), \quad (24)$$

where $\mathcal{F}_z\Pi(u, v)$ is the Fresnel transform of a square aperture, which can be expressed in terms of the special functions $\int \sin\theta^2\, d\theta$ and $\int \cos\theta^2\, d\theta$. Figure 2 illustrates a scheme that first decomposes the pupil into Fourier series, propagates each component analytically, and recombines them according to equation (23). Consequently, we have reduced the propagation of an arbitrary apodized pupil to one oscillatory integral that is the Fresnel integral for an open square aperture. Putting equations (19) and (24) together, we can obtain a final analytical expression for $E_z(u, v)$.

This expansion of the apodization function can be very useful in the practical case of finite optics, for which Theorem 1 does not hold exactly. Because it is based on well-known tabulated functions, it provides a quick method to numerically evaluate a relationship between oversizing of the optics and contrast degradation due to Fresnel effects.

3. EVALUATION OF CONTRAST DEGRADATION IN THE CASE OF FINITE OPTICS

Theorem 1 states that in the case of infinite optics, $\mathcal{F}_z\mathcal{A}(u, v)$ can be replaced by $A(u, v)$ in Theorem 2 without any consequence to the contrast level. However, practical implementation of a coronagraph requires finite optics, though ones that are generally oversized compared with the size of the pupil. The purpose of this section is to study the effect of this field truncation and to derive an upper bound, which is a function of the oversizing, for the contrast degradation due to these propagation effects. Suppose the optics are oversized by a factor of γ compared with the size of the pupil. Then the truncated, propagated field is given by

$$[\mathcal{F}_z\mathcal{A}(u,v)]_{\gamma D} = \Pi_{\gamma D}(u,v)\sum_{m,n} a^0_{m,n}e^{-i\pi\lambda z(n^2+m^2)/D^2}e^{i2\pi(nu+mv)/D}\mathcal{F}_z\Pi_D\left(u-\frac{n\lambda z}{D}, v-\frac{m\lambda z}{D}\right). \quad (25)$$

This pupil field yields the following image-plane distribution:

$$\widehat{[\mathcal{F}_z\mathcal{A}(u,v)}(\sigma,\tau)]_{\gamma D} = \sum_{m,n} a^0_{m,n}e^{-i\pi\lambda z(n^2+m^2)/D^2}\,\mathrm{FT}\left[\Pi_{\gamma D}(u,v)e^{i2\pi(nu+mv)/D}\mathcal{F}_z\Pi_D\left(u-\frac{n\lambda z}{D}, v-\frac{m\lambda z}{D}\right)\right](\sigma,\tau).$$

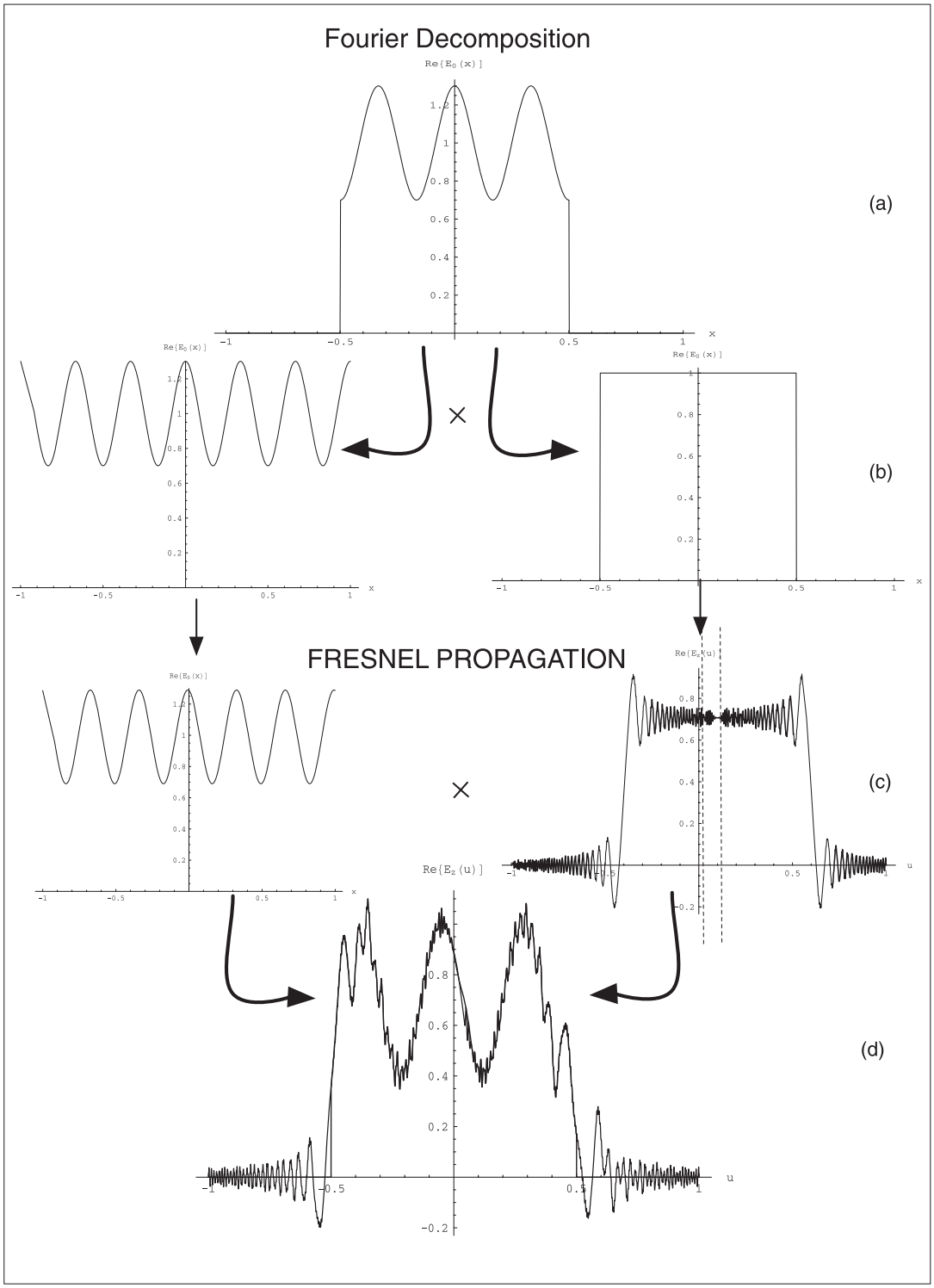

FIG. 2.— Illustration of the Fresnel propagation of a arbitrary pupil using Fourier decomposition. (*a*) Decomposition of the apodization function into a Fourier series truncated by a top-hat function. (*b*) Separation of the harmonic component and the top-hat function. (*c*) Separate propagation of the two components. Note that the shift in the propagated top-hat function has been exaggerated. (*d*) Recombination and summation in order to obtain $E_z(u, v)$. As shown in § 3, this approach enables us to derive an upper bound on propagation errors. Moreover, it provides a scheme to compute Fresnel transforms semianalytically with all the edge propagation effects included in $\mathcal{F}_z\Pi(u, v)$.

In order to quantify the error due to truncation of the propagated field, this distribution is compared with the ideal one for infinite optics:

$$[\widehat{\mathcal{F}_z\mathcal{A}(u,v)}(\sigma,\tau)]_{\gamma D} - e^{-i\pi\lambda z(\sigma^2+\tau^2)}\hat{A}(\sigma,\tau)$$
$$= \sum_{m,n} a^0_{m,n} e^{-i\pi\lambda z(n^2+m^2)/D^2}\,\mathrm{FT}\left\{[1-\Pi_{\gamma D}(u,v)]e^{i2\pi(nu+mv)/D}\mathcal{F}_z\Pi_D\left(u-\frac{n\lambda z}{D}, v-\frac{m\lambda z}{D}\right)\right\}(\sigma,\tau).$$

We now show that these errors can be bounded by a small number and thus be treated as any other wavefront aberration. Each term in the summation can be isolated and simplified using the Fourier shift theorem:

$$e^{-i\pi\lambda z(n^2+m^2)/D^2}\mathrm{FT}\left\{[1-\Pi_{\gamma D}(u,v)]e^{i2\pi(nu+mv)/D}\mathcal{F}_z\Pi_D\left(u-\frac{n\lambda z}{D},v-\frac{m\lambda z}{D}\right)\right\}(\sigma,\tau)$$
$$=\mathrm{FT}\left\{[1-\Pi_{\gamma D}(u,v)]e^{i2\pi(nu+mv)/D}\mathcal{F}_z\Pi_D(u,v)\right\}(\sigma,\tau). \quad (26)$$

To compute a tractable metric associated with Fresnel propagation errors, we will for each term of this sum integrate the energy in a finite region of the image plane $\mathcal{R}_{m,n}$ around the core of the shifted pattern associated with a given spatial frequency:

$$\int_{\mathcal{R}_{m,n}}\left|\mathrm{FT}\left\{[1-\Pi_{\gamma D}(u,v)]e^{i2\pi(nu+mv)/D}\mathcal{F}_z\Pi_D(u,v)\right\}(\sigma,\tau)\right|^2 d\sigma\,d\tau$$
$$=\int_{\mathcal{R}_{0,0}}\left|\mathrm{FT}\left\{[1-\Pi_{\gamma D}(u,v)]\mathcal{F}_z\Pi_D(u,v)]\right\}(\sigma,\tau)\right|^2 d\sigma\,d\tau, \quad (27)$$

where $R_{0,0}$ is a region of the same size as $\mathcal{R}_{m,n}$ centered around the core of the non-aberrated PSF. Finally, we use this change of variable for each term in the summation and use a squared version of the triangle inequality to derive an upper bound for the error due to the propagation of the apodization,

$$\int_{\mathcal{R}_{0,0}}\left|[\widehat{\mathcal{F}_z\mathcal{A}}(\sigma,\tau)]_{\gamma D}-e^{-i\pi\lambda z(\sigma^2+\tau^2)}\hat{A}(\sigma,\tau)\right|^2 d\sigma\,d\tau$$
$$\le 2\sum_{m,n}|a^0_{m,n}|^2\int_{\mathcal{R}_{0,0}}\left|\mathrm{FT}\left\{[1-\Pi_{\gamma D}(u,v)]\mathcal{F}_z\Pi_D(u,v)\right\}(\sigma,\tau)\right|^2 d\sigma\,d\tau$$
$$=\epsilon_{\mathrm{Fres}}(\gamma,D,z)T_0, \quad (28)$$

where we have used Parseval's theorem applied to the Fourier expansion of the aberration to replace $\sum_{m,n}|a^0_{m,n}|^2$ by T_0, the Airy throughput of the apodization. Consequently, we have derived an easily computed bound for errors induced by the propagation and truncation of the apodization function. Figure 3 shows the results of computing $\epsilon_{\mathrm{Fres}}(\gamma, D, z)$ as a function of the oversizing parameter and the propagation distance. The error is an increasing function of the propagation distance z and a decreasing function of the oversizing coefficient γ. For γ larger than 5, the bound reaches a plateau close to a 10^{-10} error. While this is only a bound and the same calculation should be carried out without using the triangle argument, it is sufficient to prove that with sufficiently oversized optics, errors due to propagation of the apodization are below the target contrast. From now on, we will assume that the optics are large enough that we can safely substitute $\mathcal{F}_z\mathcal{A}(u, v) = A(u, v)$ without altering the final results.

4. WAVELENGTH EXPANSION OF THE PROPAGATED FIELD

In order to correct for the propagated wavefront errors in equation (22) using a wavefront actuator located right before the last imaging element, one first needs to understand the real/imaginary nature of this wavefront and its wavelength dependence. This is the topic of this section, where we seek a wavelength expansion of the Fourier coefficients of a wavefront that has been reflected by several optics and gone through several propagations. The following section will show how wavefront actuators involving several DMs present a wavelength dependence that can perfectly cancel the lower order terms of this λ-Fourier expansion and thus yield a polychromatic high-contrast image. Current experiments use only one DM to correct for both amplitude and phase monochromatically. Indeed, Noecker et al. (2003) and Give'on et al. (2003) solved the real/imaginary uncertainty by showing, using symmetry considerations, that a DM, a phase-only actuator, could correct for amplitude errors by creating a dark hole in one half of the final image plane. While elegant, this method does not take full advantage of the actuator density, N actuators per unit of surface, of the DM, since the total size of the dark hole is limited to $N\lambda/4D$, half the size possible if the DM were only correcting for phase errors. Of more critical importance is the wavelength dependence of this actuator: it can only correct for $(1/\lambda)$-dependent phase errors and thus cannot perfectly compensate for amplitude errors polychromatically.

The approach presented in this paper is of tremendous usefulness when it comes to generalizing this first generation of algorithms to polychromatic light. In order to understand the chromatic behavior of the field in plane P_b, we will proceed through a systematic λ-expansion of equation (22). To do so, we discard the linearity approximations made in § 2.

4.1. *Wavelength Expansion before Propagation*

In this section, we relax our rather strong assumptions on the size of the phase-only wavefront error to derive a more general expression that includes both amplitude and phase errors. Consider the case of an aberration in phase and reflectivity in an unpropagated pupil plane:

$$E_0(x,y)=A(x,y)[1+r(x,y)]e^{i\phi(x,y)}. \quad (29)$$

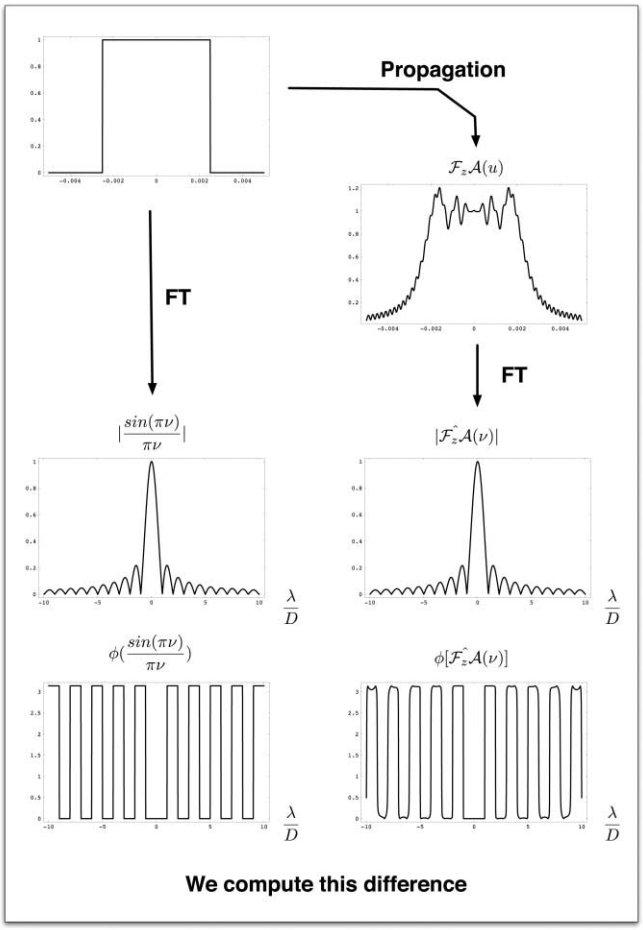

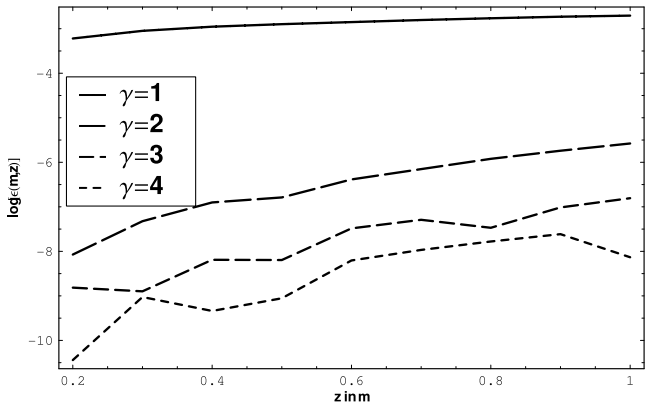

FIG. 3.—Upper limit for the contrast degradation due to Fresnel effects, as a function of the propagation distance. *Right*, the numerical scheme used to compute the bound; *left*, results for a 5 mm pupil. This size was chosen in order to obtain a proper sampling of the propagated field using reasonably sized arrays. For $\gamma > 5$, the error due to propagation of the apodization is below 10^{-10}. Since Fresnel effects are a decreasing function of the pupil size, this result can be generalized to larger pupils. [*See*

The amplitude and the phase error can each be expanded in a Fourier series,

$$r(x,y) = \sum_{m,n} a_{m,n} e^{i2\pi(mx+ny)/D}, \qquad \phi(x,y) = \sum_{m,n} \frac{2\pi b_{m,n}\lambda_0}{\lambda} e^{i2\pi(mx+ny)/D} \tag{30}$$

with $a_{-m,-n} = a^*_{m,n}$ and $b_{-m,-n} = b^*_{m,n}$. The $b_{m,n}$ are again dimensionless coefficients that represent the phase shift introduced by a surface corrugation of one of the optics at the wavelength λ_0. When the illumination wavelength is such that $\lambda > \lambda_0$, this phase shift decreases. We then take a Taylor expansion of the exponential, as suggested by Give'on et al. (2006):

$$e^{i\phi(x,y)} = 1 + i\sum_{m,n} \frac{2\pi b_{m,n}\lambda_0}{\lambda} e^{i2\pi(mx+ny)/d} - \sum_{m,n}\sum_{p,q} \frac{4\pi b_{m,n} b_{p,q}\lambda_0^2}{\lambda^2} e^{i2\pi[(m+p)x+(n+q)y]/D} + O(b^3_{m,n}), \tag{31}$$

where we have only shown the first three terms. Despite the complex notation chosen for our Fourier coefficients, we can show that the second-order term is real. To see this, we can come back to the expression before the expansion, where ϕ is real,

$$e^{i\phi} = 1 + i\phi - \frac{\phi^2}{2} + \cdots + i^l \frac{\phi^l}{l!} + \cdots. \tag{32}$$

Consequently, the odd terms are imaginary and the even terms are real. This expression for the phase is then plugged into the field distribution at the pupil:

$$[1 + r(x,y)]e^{i\phi(x,y)} = 1 + \sum_{m,n} a_{m,n} e^{i2\pi(mx+ny)/D} + i\sum_{m,n} \frac{2\pi b_{m,n}\lambda_0}{\lambda} e^{i2\pi(mx+ny)/D}$$
$$+ i\sum_{m,n}\sum_{p',q'} \frac{2\pi b_{m,n} a_{p,q}\lambda_0}{\lambda} e^{i2\pi[(m+p)x+(n+q)y]/D} - \sum_{m,n}\sum_{p',q'} \frac{4\pi b_{m,n} b_{p,q}\lambda_0^2}{\lambda^2} e^{i2\pi[(m+p)x+(n+q)y]/D} + O(b^3_{m,n}).$$

Consequently, this field distribution can be written as

$$E_0(x,y) = A(x,y)\left(1 + \sum_{m,n}\sum_{k>1} i^k \frac{c_{m,n}^{-k}\lambda_0^k}{\lambda^k} e^{i2\pi(mx+ny)/D}\right), \tag{33}$$

where $c_{m,n}^0 = a_{m,n}$, $c_{m,n}^{-1} = b_{m,n} + \sum_{p,q} a_{p,q} b_{m-p,n-q}$, $c_{m,n}^{-2} = \sum_{p,q} b_{p,q} b_{m-p,n-q}$, and $c_{m,n}^{-3} = O(b_{m,n}^3)$.

4.2. *Propagation of This Expansion*

Once expanded, $E_0(x, y)$ in equation (33) is propagated using Theorem 2 in order to derive the distribution in plane P_z:

$$E_z(u,v) = \mathcal{F}_z\mathcal{A}(u,v) + \sum_{m,n}\sum_{k>0} i^k \frac{c_{m,n}^{-k}\lambda_0^k}{\lambda^k} e^{-i\pi\lambda z(n^2+m^2)/D^2} e^{i2\pi(mu+nv)/D} \mathcal{F}_z\mathcal{A}\left(u - \frac{m\lambda z}{D}, v - \frac{n\lambda z}{D}\right). \tag{34}$$

Exoplanet detection only requires active correction for low-to-mid spatial frequencies, allowing us to only consider terms for which $(n, m) \ll D^2/\lambda z$ and to neglect the shift in the propagated apodization. In any case, the angular spectrum factor can be written as a Taylor series:

$$e^{-i\pi\lambda z(m^2+n^2)/D^2} = 1 + \sum_{p>0} \frac{1}{p!}\left[-i\frac{\pi\lambda z(m^2+n^2)}{D^2}\right]^p. \tag{35}$$

Substituting this into the (m, n)-term in equation (34) yields

$$\sum_{k>0} i^k \frac{c_{m,n}^{-k}}{\lambda^k} \sum_{p>0} \frac{1}{p!}\left[-i\frac{\pi\lambda z(n^2+m^2)}{D^2}\right]^p = \sum_{\substack{k>0\\p>0}} \frac{(-1^p)}{p!} i^{k-p} \frac{c_{m,n}^{-k}\lambda_0^k}{\lambda^{k-p}} \left[\frac{\pi z(m^2+n^2)}{D^2}\right]^p. \tag{36}$$

By changing the index in the wavelength series, the field in plane P_z can be expressed through the following λ-Fourier expansion:

$$E_z(u,v) = \mathcal{F}_z\mathcal{A}(u,v)\left(1 + \sum_{m,n}\sum_{k=-\infty}^{+\infty} i^k \frac{d_{m,n}^{-k}\lambda_0^k}{\lambda^k} e^{i2\pi(mu+nv)/D}\right), \tag{37}$$

where again $d_{-m,-n} = d_{m,n}^*$. These coefficients can be related to the Fourier coefficients of the initial aberration. Since there are three small quantities in this expansion, $a_{m,n}$, $b_{m,n}$, and $\pi\lambda_0 z(n^2 + m^2)/D^2$, we can write the orders around $k = 0$ as follows:

$$k = -2: \quad \lambda^2: \quad d_{m,n}^2 = O\left(a_{m,n}\left(\pi z\lambda_0 \frac{n^2+m^2}{D^2}\right)^2\right), \tag{38a}$$

$$k = -1: \quad i\lambda^1: \quad d_{m,n}^1 = \frac{\pi z\lambda_0(n^2+m^2)}{D^2} a_{m,n} + O\left(b_{m,n}\left(\pi z\lambda_0 \frac{n^2+m^2}{D^2}\right)^2\right), \tag{38b}$$

$$k = 0: \quad \lambda^0: \quad d_{m,n}^0 = a_{m,n} - \frac{4\pi^2 z\lambda_0(n^2+m^2)}{D^2} b_{m,n}(1 + a_{m,n}) + O\left(b_{m,n}^2\left(\pi z\lambda_0 \frac{n^2+m^2}{D^2}\right)^2\right), \tag{38c}$$

$$k = 1: \quad i\lambda^{-1}: \quad d_{m,n}^{-1} = 2\pi b_{m,n}(1 + a_{m,n}) + O\left(b_{m,n}^2 \pi z\lambda_0 \frac{n^2+m^2}{D^2}\right), \tag{38d}$$

$$k = 2: \quad \lambda^{-2}: \quad d_{m,n}^{-2} = (2\pi b_{m,n})^2 + O\left(b_{m,n}^3 \pi\lambda_0 z \frac{n^2+m^2}{D^2}\right), \tag{38e}$$

$$k = 3: \quad i\lambda^{-3}: \quad d_{m,n}^{-3} = O(b_{m,n}^3). \tag{38f}$$

In the image plane, the field distribution will consist of shifted copies of the PSF. The intensity due to a given pupil-based spatial frequency is

$$I_{m,n}(\sigma,\tau) = |\mathcal{F}_z\mathcal{A}(\sigma - m, \tau - n)|^2 \left|\sum_{k=-\infty}^{+\infty} i^k \frac{d_{m,n}^{-k}\lambda_0^k}{\lambda^k}\right|^2. \tag{39}$$

Thus, we quantify the efficiency of different wavefront correction algorithms by computing the magnitude of the coefficient weighting the shifted PSF:

$$I_{m,n}(\lambda) = \left(\sum_{k\ \text{even}} \frac{d_{m,n}^{-k}\lambda_0^k}{\lambda^k}\right)^2 + \left(\sum_{k\ \text{odd}} \frac{d_{m,n}^{-k}\lambda_0^k}{\lambda^k}\right)^2. \tag{40}$$

Consequently, the dominant terms in the $d_{m,n}$ expansion derived above are mainly responsible for the contrast degradation due to propagated aberrations. Note that because of speckle-speckle E-field interactions, $I_{m,n}(\lambda)$ is not rigorously the value of the intensity distribution at any point in the image plane. However, it provides a useful metric that immediately translates our λ-Fourier expansion into contrast.

4.3. *Generalization to Multiple Optics*

The goal of any wavefront actuator is to reduce intensity error below 10^{-10} of the peak. For instance, assume that there is a deformable mirror right before the final imaging element and that it acts as a controllable phase actuator, modifying the imaginary, $(1/\lambda)$-dependent part of the field distribution. To relate the effect of a deformation to equation (37), one can see that it can correct only for the $i d_{m,n}^{-1}\lambda_0/\lambda$ part of the λ-Fourier expansion. Of course, it has been extensively proved in the literature that it can perfectly cancel for all the terms in this expansion under monochromatic illumination. In polychromatic light, however, a residual halo appears. To see this, we place a DM in plane P_z and obtain the field distribution at this plane,

$$E_z(u,z) = \mathcal{F}_z\mathcal{A}(u,v)\left[1 + \sum_{m,n}\left(\sum_{k>0} i^k \frac{d_{m,n}^{-k}\lambda_0^k}{\lambda^k} e^{-i\pi\lambda_0 z(n^2+m^2)/D^2} - i\frac{b_{m,n}^{\mathrm{DM}}\lambda_0}{\lambda}\right)e^{i2\pi(mu+nv)/D}\right], \tag{41}$$

where the Fourier coefficients of the aberration are composed of two terms: a sum corresponding to the propagation aberration, and an i/λ term that is the effect of the DM, the $b_{m,n}^{\mathrm{DM}}$ being the Fourier coefficients of the DM surface. In this configuration, choosing

$$b_{m,n}^{\mathrm{DM}+} = \sum_k \frac{d_{m,n}^{-k}}{\lambda_0^k} \quad \text{if } m > 0 \text{ for all } n, \qquad b_{m,n}^{\mathrm{DM}-} = -(b_{m,n}^{\mathrm{DM}+})^* \quad \text{if } m < 0 \text{ for all } n \tag{42}$$

leads to a perfect extinction at $\lambda = \lambda_0$ and a residual halo under polychromatic illumination. Better broadband performance could be obtained with one DM, assuming that the imaging optics are separated from plane P_z by a distance z_{DM}. Then the field at the location of the final lens would be

$$E_{z+z_{\mathrm{DM}}}(u,z) = \mathcal{F}_{z+z_{\mathrm{DM}}}\mathcal{A}(u,v)\left[1 + \sum_{m,n}\left(\sum_{k>0} i^k \frac{d_{m,n}^{-k}\lambda_0^k}{\lambda^k} e^{-i\pi\lambda_0 z(n^2+m^2)/D^2} - i\frac{b_{m,n}^{\mathrm{DM}}\lambda_0}{\lambda} e^{-i\pi\lambda z_{\mathrm{DM}}(n^2+m^2)/D^2}\right)e^{i2\pi(mu+nv)/D}\right],$$

where the DM surface expansion has been propagated as in the previous section. Then, by adequately choosing $b_{m,m}^{\mathrm{DM}}$ and z_{DM}, all the terms with $k > 0$ and that depend on $b_{m,n}$ in equations (38a)–(38f) would be canceled, and the broadband performance, while still not perfect, would be considerably enhanced. Another way to state this feature is that propagated phase errors can be corrected broadband using a DM in a plane that is conjugate to the initial pupil. However, there is an important caveat: if the optical train of a telescope reflects off several mirrors and undergoes multiple propagations, implementing such a correction scheme would imply one DM per aberrated optic. This would prohibitively increase the cost and the reliability of the system. For the remainder of this work we will discard this solution and, instead, focus on finding an analytical expression for the field distribution after multiple propagations that is of the form of equation (37). The following theorem states such a result:

THEOREM 3. *Assuming that the optics are sufficiently oversized in the sense of § 3, and dealing with spatial frequencies such that* $(m, n) \ll D^2/\lambda z$, *the field in any plane of the optical train of a telescope, after an arbitrary number of reflections on aberrated optics and propagations, can be expanded using the following λ-Fourier expansion:*

$$E(u,v) = A(u,v)\left(1 + \sum_{m,n}\sum_k i^k \frac{f_{m,n}^{-k}\lambda_0^k}{\lambda^k} e^{i2\pi(mu+nv)/D}\right), \tag{43}$$

where $f_{-m,-n}^{-k} = (f_{m,n}^{-k})^*$. *That is, the odd terms in the wavelength expansion are imaginary and the even terms are real.*

Proof. We proved in the previous subsection that this property is true for one propagation. We will thus proceed by induction. Assuming that equation (43) is true after P propagations and that the resulting field lands on aberrated optics with an amplitude error given by an $a_{m,n}^{(P+1)}$ series and a phase error by a $b_{m,n}^{(P+1)}$ series, the field is then propagated over a distance z_{P+1}. Since we assume that the property is true for P propagations, the field $E_{z_P}(x, y)$ admits an expansion that has the form of equation (43), with an $f_{m,n}^{(P),-k}$ series. The $P + 1$ aberrated optic introduces errors that can be collected together in a λ-Fourier series as

$$\frac{E_{z_P,R}(u,v)}{E_{z_P}(u,v)} = 1 + \sum_{m,n}\sum_{k>0}\frac{c_{m,n}^{(P+1),-k}\lambda_0^k}{\lambda^k} e^{i2\pi(mu+nv)/D}. \tag{44}$$

The reflected field is the product of the $f_{m,n}^{(P),-k}$ series and the $c_{m,n}^{(P+1),-k}$ series:

$$E_{z_P,R}(u,v) = \mathcal{F}_{z_P}\mathcal{A}(u,v)\left[1 + \sum_{m,n}\sum_{\substack{k\neq 0\\ l>1}}\left(i^k\frac{f_{m,n}^{(P),-k}\lambda_0^k}{\lambda^k} + i^l\frac{c_{m,n}^{(P+1),-l}\lambda_0^l}{\lambda^l}\right)e^{i2\pi(mu+nv)/D} + \sum_{m,n}\sum_{p,q}\sum_{\substack{k\neq 0\\ l>1}} i^{k+l}\frac{f_{m,n}^{(P),-k}c_{p,q}^{(P+1),-l}\lambda_0^{k+l}}{\lambda^{k+l}} e^{i2\pi[(m+p)u+(n+q)v]/D}\right]. \tag{45}$$

The first term presents the property of equation (43), since it is a linear combination of terms that satisfy it. A more careful look at the summation associated with the cross product shows that it exhibits an i^{k+l}/λ^{k+l} dependence that satisfies equation (43) as well. Thus, we can put all the coefficients with the same λ-dependence together and write

$$E_{z_P,R}(u,v) = \mathcal{F}_{z_P}\mathcal{A}(u,v)\left(1 + \sum_{m,n}\sum_{k\neq 0} i^k \frac{g_{m,n}^{(P+1),-k}\lambda_0^k}{\lambda^k} e^{i2\pi(mu+nv)/D}\right). \tag{46}$$

Finally, this result can be propagated another time. Using Theorem 2, and neglecting the $m\lambda z/D$ shifts, we find

$$E_{z_P,R,z_{P+1}}(u,v) = \mathcal{F}_{z_{P+1}}[\mathcal{F}_{z_P}\mathcal{A}(u,v)]\left(1 + \sum_{m,n}\sum_{k\neq 0} i^k \frac{g_{m,n}^{(P+1),-k}\lambda_0^k}{\lambda^k} e^{i\pi\lambda z_{P+1}(m^2+n^2)/D^2} e^{i2\pi(mu+nv)/D}\right). \tag{47}$$

Using Corollary 1 and the fact that the optics are oversized in the sense of § 3, we can write $\mathcal{F}_{z_{P+1}}[\mathcal{F}_{z_P}\mathcal{A}(u,v)] = A(u,v)$ and include the tiny contrast degradation due to the propagation of the apodization in the wavefront error. Taking a Taylor expansion of the z_{P+1}-dependent angular spectrum factor, as carried out in detail in the previous section, leads to an expansion in the form of equation (43). □

This result highlights a fundamental property that a DM-based wavefront actuator must exhibit in order to correct propagated wavefronts under broadband. That is, in order to eliminate one given term in the λ-Fourier expansion, the actuator has to exhibit a controllable mode that behaves as i^k/λ^k. For the purpose of this work, we only focus on actuators that correct for terms that are of the first or second order in $a_{m,n}$, $b_{m,n}$, and $\pi\lambda_0 z(n^2+m^2)/D^2$. Indeed, typical values of these dimensionless quantities are between 10^{-2} and 10^{-3}. Third-order terms would yield a residual intensity always below 10^{-12}. As shown in equations (38a)–(38f), this corresponds to correcting for the $f_{m,n}^0$, $f_{m,n}^{-1}$, and $f_{m,n}^{-2}$ terms. Note that while $f_{m,n}^1$ is also a second-order term, it yields a residual halo below 10^{-10} for projected values of the reflectivity errors, so we will not attempt to correct for it.

5. CORRECTION SCHEMES USING MULTIPLE DEFORMABLE MIRRORS

5.1. *Monochromatic Dark Hole*

Malbet et al. (1995) presented a numerical proof of the feasibility of a DM to generate a high-contrast dark hole in the image plane of a telescope. Recent works (referenced above) have refined this idea and proved that a contrast of 10 orders of magnitude could be obtained monochromatically. While these algorithms create a dark hole for a given wavelength, contrast is degraded when bandwidth increases. This is illustrated in Figure 4 (*top left*), where one DM has been set up to correct perfectly for all the aberrations at $\lambda_0 = 600$ nm. This corresponds to setting the DM to the deformation shown in equation (42). Then, by plugging this deformation into equation (41), the residual halo $I_{m,n}(\lambda)$, introduced in equation (40), can be evaluated and integrated over the bandwidth $\Delta\lambda$,

$$I_{m,n}^{\mathrm{DH}} = \frac{1}{\Delta\lambda}\int_{\Delta\lambda}\left|\sum_k i^k f_{m,n}^{-k}\frac{\lambda_0^k}{\lambda^k} - i b_{m,n}^{\mathrm{DM}}\frac{\lambda_0}{\lambda}\right|^2 d\lambda \simeq \frac{a_{m,n}^2}{\Delta\lambda}\int_{\lambda_0-\Delta\lambda/2}^{\lambda_0+\Delta\lambda/2}\left(1-\frac{\lambda_0}{\lambda}\right)^2 d\lambda. \tag{48}$$

The $f_{m,n}^0 \simeq a_{m,n}$ term in the λ-Fourier expansion is then primarily responsible for the residual polychromatic halo.

Unfortunately, this approach ignores any knowledge of the wavelength dependence of the aberrated wavefront. In this section we will assume that there exists an estimation scheme for the coefficients $f_{m,n}^k$, discriminating the different λ-dependences for each spatial frequency. For the remainder of this section, we focus on methods that use this knowledge in order to create a polychromatic null that does not vary with bandwidth.

5.2. *Monochromatic Phase Conjugation*

We first assume a single deformable mirror and consider a phase-only control algorithm that sets the DM such that only the $f_{m,n}^{-1}$ coefficients, which behave as i/λ, are canceled:

$$b_{m,n}^{\mathrm{DM}} = -f_{m,n}^{-1}. \tag{49}$$

Since this approach does not attempt to correct any of the other wavelength-dependent terms, it is chromatic and behaves worse than the dark-hole approach under a narrow band. Nevertheless, we include it here because it has the merit of presenting a contrast leakage that can be easily linked to second-order phenomena. Indeed, after such a correction there are three dominant sources of contrast degradation that are of the same order of magnitude: reflectivity nonuniformities and phase-induced amplitude errors, which are both contained in $f_{m,n}^0$, and second-order phase errors due to frequency folding, the leading term of $f_{m,n}^{-2}$. The residual intensity after correction is thus

$$I_{m,n}^{\mathrm{PC}} = \frac{1}{\Delta\lambda}\int_{\Delta\lambda}\left|\sum_{k\neq 1} i^k f_{m,n}^{-k}\frac{\lambda_0^k}{\lambda^k}\right|^2 d\lambda \simeq I_{m,n}^{\mathrm{PC},0} + I_{m,n}^{\mathrm{PC},-2} + O(b_{m,n}^6), \tag{50}$$

where $I_{m,n}^{\mathrm{PC},0}$ corresponds to the wavelength-independent part of the residual halo,

$$I_{m,n}^{\mathrm{PC},0} = \frac{1}{\Delta\lambda}\int_{\Delta\lambda}\left\{a_{m,n}^2 + \left(\frac{2\pi b_{m,n}\lambda_0}{\lambda}\right)^2\left[\frac{\pi z(m^2+n^2)\lambda}{D}\right]^2\right\} d\lambda, \tag{51}$$

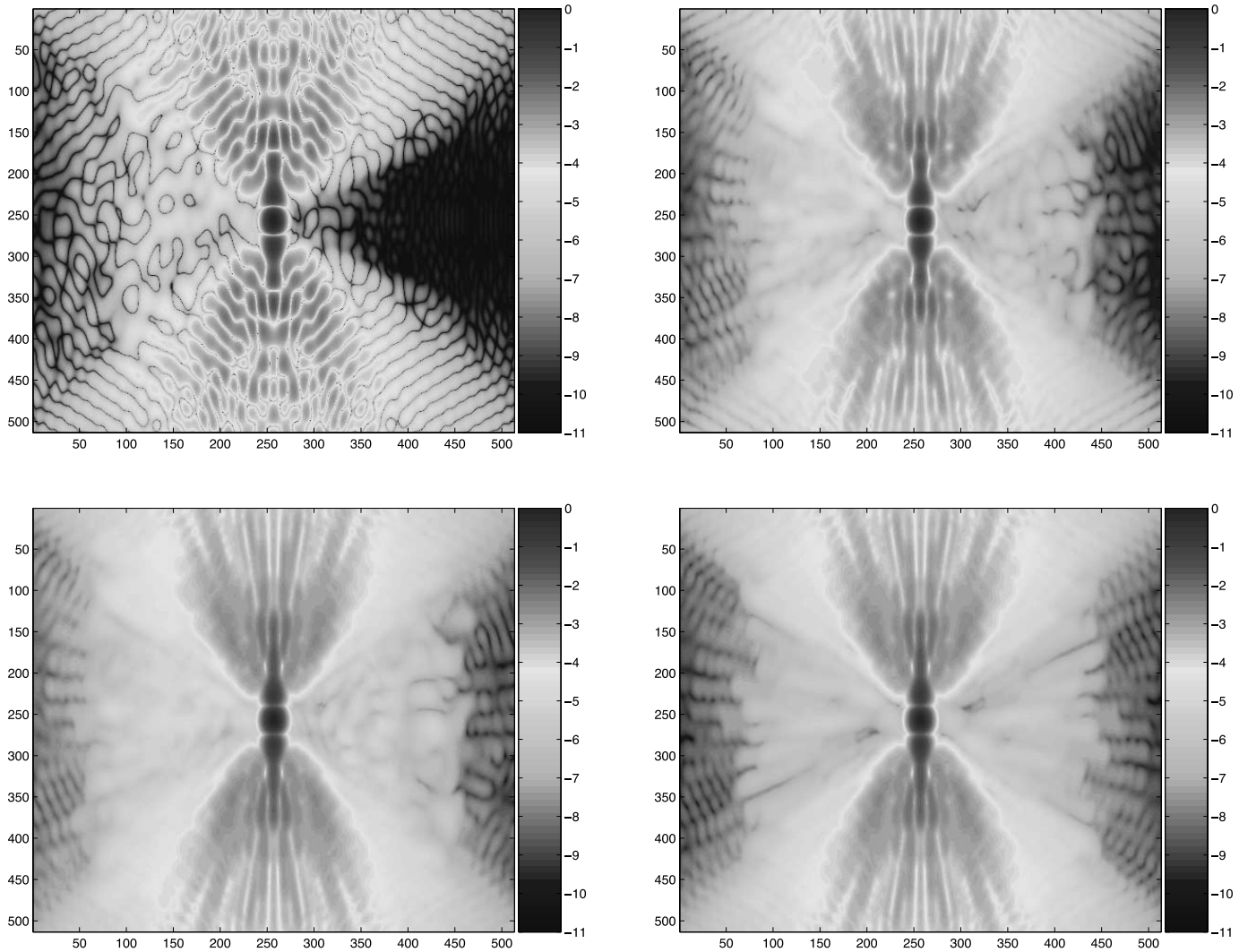

FIG. 4.—Simulations of the effects in the image plane of several wavefront corrections with one DM. We created the aberration by randomly generating the coefficients of the three leading terms of the λ-Fourier expansion, $\{f^0_{m,n}, f^{-1}_{m,n}, f^{-2}_{m,n}\}$. Their rms values were chosen arbitrarily as $\{10^{-3}, 10^{-2}, 10^{-4}\}$. We assumed a perfect deformable mirror that can correct any deformation and a perfect estimator that provides adequate control signals to the DM. *Top left*, dark-hole (DH) algorithm, $\Delta\lambda = 0$ nm; *top right*, DH algorithm, $\Delta\lambda = 200$ nm; *bottom left*, DH algorithm, $\Delta\lambda = 400$ nm; *bottom right*, phase conjugation, $\Delta\lambda = 400$ nm. A dark-hole algorithm perfectly corrects for all the aberration only for the central wavelength λ_0. [*See the electronic edition of the Journal for a color version of this figure.*]

and $I^{\mathrm{PC},-2}_{m,n}$ corresponds to the $1/\lambda^2$, frequency-folding, component of that residual wavefront,

$$I^{\mathrm{PC},-2}_{m,n} = \frac{1}{\Delta\lambda}\int_{\Delta\lambda}\left(\frac{4\pi^2 b_{k,l} b_{p,q}\lambda_0^2}{\lambda^2}\right)^2 d\lambda, \tag{52}$$

with $n = k - p$ and $m = l - q$ as presented by Give'on et al. (2006). In an effort to reduce the polychromatic halo below I^{DH}, the remainder of this paper will consider the addition of several DMs and prove that polychromatic starlight extinction is feasible. The next subsection shows how wavelength-independent aberrations, responsible for $I^{\mathrm{PC},0}$, can be canceled, followed by the case of $1/\lambda^2$ errors.

5.3. *Amplitude Correction Using Two Cascaded Deformable Mirrors*

Wavelength-independent aberrations, given by $f^0_{m,n}$, are the main source of contrast degradation once phase errors have been corrected. They arise from two separate phenomena: reflectivity nonuniformity and phase-induced errors due to Fresnel propagation. Shaklan & Green (2006) first realized that this second effect could be used to our advantage as far as wavefront stability is concerned. Consider two DMs separated by a large distance z_{DM}, as shown in Figure 5. The Fourier coefficients of the deformation of the two deformable mirrors are written as $b^{\mathrm{DM1}}_{m,n}$ and $b^{\mathrm{DM2}}_{m,n}$, and we assume that their reflectivity is uniform. Then, using Theorem 3, we can show that the field right after the second DM is given by equation (43). One can then prove that the leading terms of this expansion are

$$f^{(\mathrm{2DM},0)}_{m,n} = \frac{2\pi^2 z_{\mathrm{DM}}(m^2+n^2)}{D^2} b^{\mathrm{DM1}}_{m,n}, \qquad f^{(\mathrm{2DM},-1)}_{m,n} = 2\pi(b^{\mathrm{DM1}}_{m,n} + b^{\mathrm{DM2}}_{m,n}). \tag{53}$$

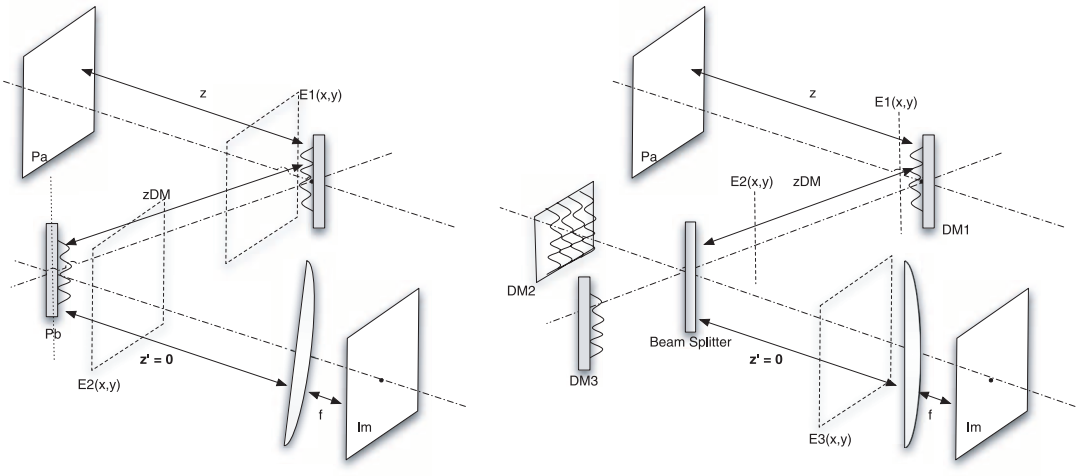

FIG. 5.—Multiple-DM setup that corrects for multiple orders in the λ-Fourier expansion. *Left*: Two sequential DMs separated by a propagation over a known distance z_{DM} can correct for $\{f^{0}_{m,n}, f^{-1}{}_{m,n}\}$. *Right*: One DM followed at the distance z_{DM} by a Michelson interferometer equipped with two other DMs can correct for $\{f^{0}_{m,n}, f^{-1}_{m,n}, f^{-2}_{m,n}\}$.

In theory, higher order coefficients could be corrected instead using the DMs; however, since we only have 2 degrees of freedom, we choose to control the largest $f^{k}_{m,n}$. Since the $k = 0$ and $k = -1$ modes in the λ-Fourier expansion of the cascaded DM setup are controllable, there exists a set of deformations that perfectly cancel them. Then the residual intensity becomes

$$I^{\mathrm{2DM}}_{m,n} = \frac{1}{\Delta\lambda}\int_{\Delta\lambda}\left|\sum_{k\neq 0,1} i^{k} f^{-k}_{m,n}\frac{\lambda_0^{k}}{\lambda^{k}}\right|^{2} d\lambda \simeq I^{\mathrm{PC},-2}_{m,n}. \tag{54}$$

This proves that two cascaded deformable mirrors can correct for imaginary $1/\lambda$ terms and real wavelength-independent terms. Simulations of such a correction are shown in Figure 6; a net gain in polychromatic contrast can be observed. After such a correction, the $1/\lambda^{2}$ aberrations, $I^{\mathrm{PC},-2}_{m,n}$, the result of frequency folding of phase errors, are responsible for the chromatic contrast floor. The following subsection shows how to reduce this floor further by using a Michelson interferometer.

5.4. *Correction of Frequency Folding Using Two Deformable Mirrors in an Interferometer*

The idea of using DMs in an interferometric configuration was first introduced by Littman et al. (2003) in order to compensate for reflectivity nonuniformities. They showed that this configuration resulted in a $1/\lambda^{2}$ dependence and thus would lead to chromatic leakage when correcting wavelength-independent errors (Pueyo et al. 2005). We propose here to take advantage of this dispersion in order to correct for errors due to frequency folding. We consider a setup with three deformable mirrors, as shown in Figure 5, that

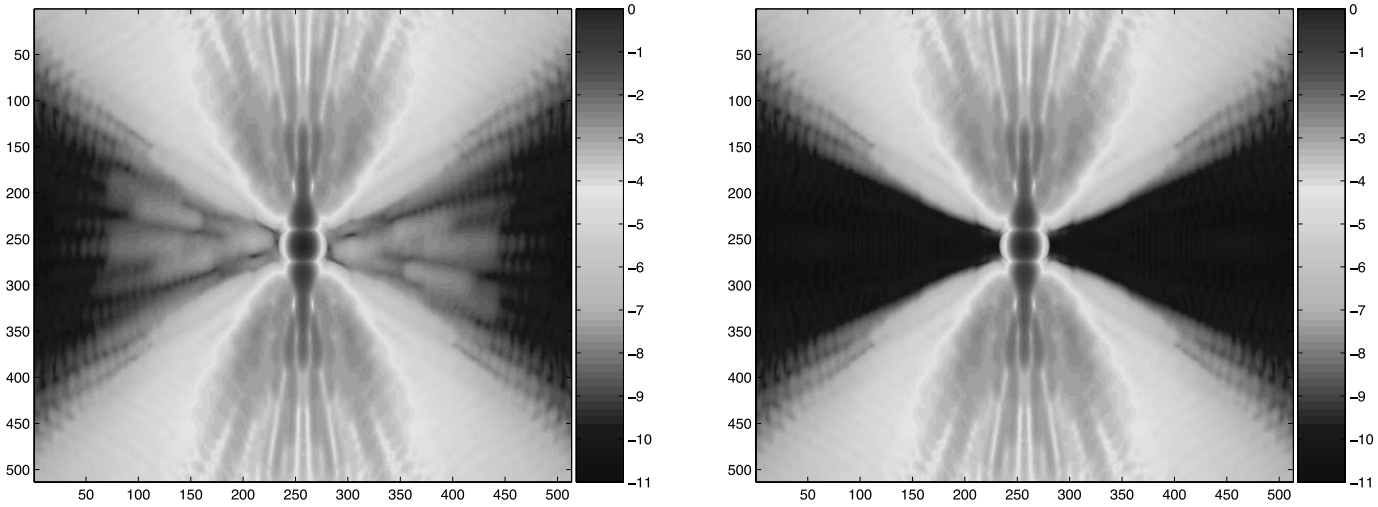

FIG. 6.— Same as Fig. 4, but for multiple DMs. *Left*: Two sequential DMs correct for phase and λ-independent errors, $\Delta\lambda = 400$ nm; a halo due to frequency-folding errors remains. *Right*: The introduction of a third DM in a Michelson configuration enables one to correct for these errors, $\Delta\lambda = 400$ nm. [*See the electronic edition of the Journal for a color version of this figure*.]

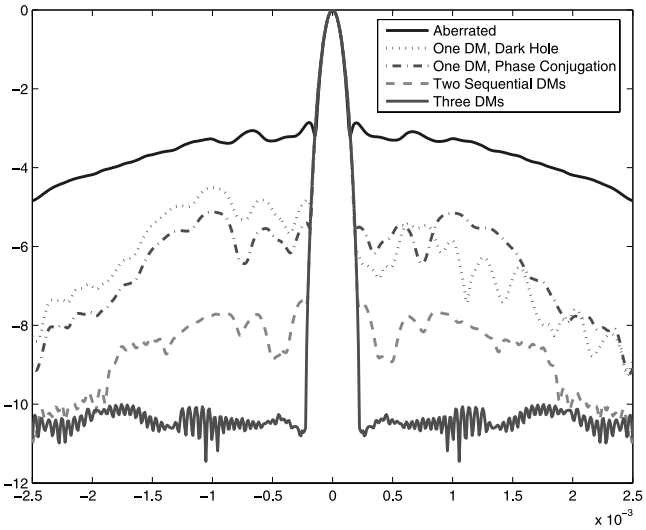

FIG. 7.—Slices of the several polychromatic PSFs presented above $\Delta\lambda = 400$ nm. Schemes involving one DM can only correct for the i/λ component of the aberration for this bandwidth: on the right, the level of the corrected PSF using a dark-hole correction is about the same as for phase conjugation. For three DMs, the leading terms of the λ-Fourier expansion can be canceled, and the ideal PSF is retrieved. [*See the electronic edition of the Journal for a color version of this figure*.]

includes an initial DM followed at a distance $z_{\rm DM}$ by a Michelson interferometer. The transfer function of the interferometer is given by

$$\frac{E_3(x,y)}{E_2(x,y)} = \cos\left\{\frac{\pi}{\lambda}\left[h_{\rm DM2}(x,y) - h_{\rm DM3}(x,y)\right]\right\} e^{i\pi[h_{\rm DM2}(x,y)+h_{\rm DM3}(x,y)]/\lambda} \tag{55}$$

$$\simeq \left(1 - \frac{1}{2}\left\{\frac{\pi}{\lambda}\left[h_{\rm DM2}(x,y) - h_{\rm DM3}(x,y)\right]\right\}^2\right) e^{i\pi[h_{\rm DM2}(x,y)+h_{\rm DM3}(x,y)]/\lambda}, \tag{56}$$

where the $h_{{\rm DM}r}(x, y)$ are the heights of the two DMs and are related to the Fourier decomposition of the phase shift through the relationship $h_{{\rm DM}r}(x, y) = \sum_{m,n} b^{{\rm DM}r}_{m,n} \lambda_0 e^{i2\pi(mx+ny)/D}$. Combining this result with Theorem 3, we can prove that the field distribution right after the beam splitter has the form of equation (43), with 3 degrees of freedom that allow correction for three wavelength orders in the $f^{-k}_{m,n}$.

$$f^{(3{\rm DM},0)}_{m,n} = \frac{2\pi^2 z_{\rm DM}(m^2+n^2)}{D^2} b^{\rm DM1}_{m,n}, \qquad f^{(3{\rm DM},-1)}_{m,n} = \pi(2b^{\rm DM1}_{m,n} + b^{\rm DM2}_{m,n} - b^{\rm DM3}_{m,n}), \tag{57}$$

$$f^{(3{\rm DM},-2)}_{m,n} = \frac{\pi^2}{2}\sum_{p,q}(b^{\rm DM2}_{p,q} - b^{\rm DM3}_{p,q})(b^{\rm DM2}_{m-p,n-q} - b^{\rm DM3}_{m-p,n-q}). \tag{58}$$

This arrangement compensates polychromatically, with three deformable mirrors, for the three main sources of contrast degradation presented above. A simulation of this polychromatic correction is presented in Figure 6. As shown in Figure 7, the slices along the high-contrast line of the PSF quantify the progression of the depth of the AO-generated null when DMs are added. The method presented here uses only three DMs, and an experimental implementation is feasible, even if the constraints on the optical design of an experimental setup are quite severe. Our approach takes optimal advantage of these 3 degrees of freedom using an a priori theoretical model to estimate the wavelength dependence of the speckle field in the presence of Fresnel propagation. The remaining terms of the expansion presented in § 3 are the source of a residual halo that can be quantified using the multiwavelength methodology presented in this paper. In a final section, we will generalize our wavefront-control scheme to systems of multiple deformable mirrors that can correct for these higher orders and show that for any number of DMs, a null can only be created up to a maximum outer working angle.

6. SURFACE REQUIREMENTS AND OUTER WORKING ANGLE LIMIT

6.1. *Surface Requirements*

As illustrated in the simulations above, adding deformable mirrors reduces the residual polychromatic halo. It is however of the utmost importance to determine how much this improvement enables us to relax the requirements on the surface and the reflectivity of the optics. That is, we wish to find the maximum magnitude of the coefficients $\{a_{m,n}, b_{m,n}\}$ of each optic for which the residual halo after correction would still be below the target contrast. Since the schemes presented in the previous section only correct for first- and second-order terms under a broadband illumination, the requirements will be driven by the higher order terms in equation (43), and the $\{a_{m,n}, b_{m,n}\}$ will be constrained under a value that would lead the polychromatic halo due to these terms to be above 10^{-10}. If the surface and reflectivity qualities achievable using a state-of-the-art manufacturing technique are within this requirement, then one can conclude

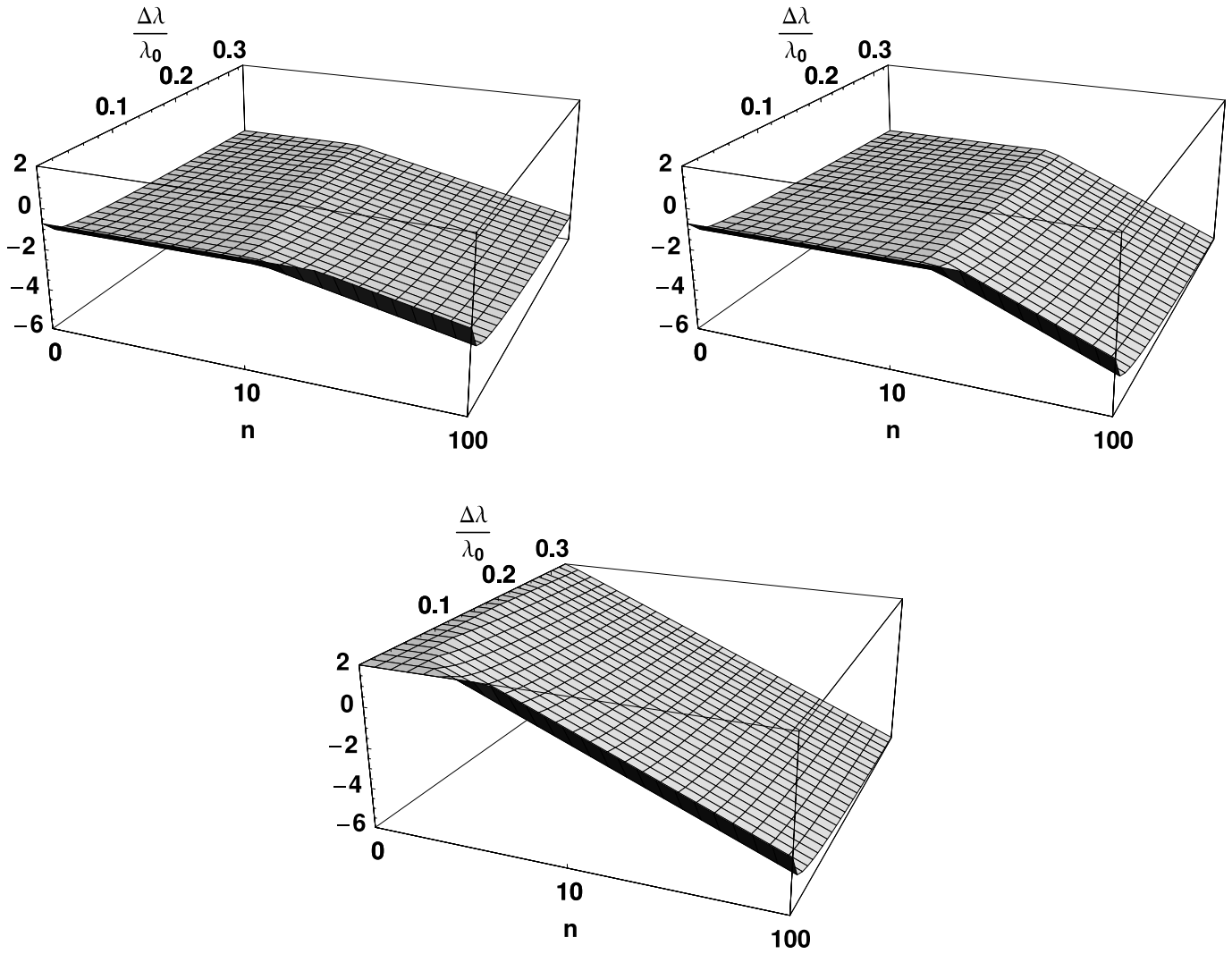

FIG. 8.— Surface requirements for a target contrast of $C = 10^{-10}$ as a function for bandwidth and spatial frequency. If the power spectral density of the optics is below this requirement, then the contrast C can be achieved after wavefront compensation. *Top left*: For a one-DM control scheme, the plateau at low spatial frequencies is due to frequency-folding errors and the slope to phase-induced amplitude errors. *Top right*: By adding one DM, sequential configuration, the phase-induced amplitude errors are corrected and consequently the requirement at high spatial frequencies is loosened; the cutoff frequency is higher. *Bottom*: The Michelson corrects for frequency-folding errors and thus the plateau disappears, relaxing the requirements even more. [*See the electronic edition of the Journal for a color version of this figure*.]

that the correction scheme is successful. In order to quantify this as a function of the bandwidth for the several DM configurations presented above, we use the same approach as in equation (48):

$$I_{m,n}^{p\ \mathrm{DMs}}(\Delta\lambda) = \frac{1}{\Delta\lambda}\int_{\Delta\lambda}\left|\sum_{k=-\infty}^{+\infty} i^k f_{m,n}^{(-k)}\frac{\lambda_0^k}{\lambda^k} - \sum_{k=-(p-1)}^{0} i^k f_{m,n}^{(\mathrm{DM},-k)}\frac{\lambda_0^k}{\lambda^k}\right|^2 d\lambda, \tag{59}$$

where p corresponds to the number of DMs used and the $\{f_{m,n}^{\mathrm{DM},-k}\}_{k=0,\ldots,p}$ are chosen such that $I_{m,n}^{p\ \mathrm{DMs}} = 0$.

Then, by constraining $I_{m,n}^{p\ \mathrm{DMs}}(\Delta\lambda) = 10^{-10}$ and writing explicitly the lowest-order terms on the right-hand side of equation (59) as a function of $b_{m,n}$ and $a_{m,n}$, one can derive the surface and reflectivity requirements associated with this level of residual intensity. Figure 8 shows level sets of the surface requirements as functions of the spatial frequency and bandwidth. As expected, the requirements are a decreasing function of the bandwidth, and they are infinite for $\Delta\lambda = 0$, which is not shown in our logarithmic stretch. When there are only two DMs, the plateau for low spatial frequencies corresponds to chromatic leakage due to frequency-folding errors. Note that adding cascaded DMs relaxes the contrast for low spatial frequencies but makes the slope of these requirements steeper. Thus, when the target contrast is 10^{-10}, for sufficiently high spatial frequency the surface requirement with multiple DMs becomes tighter than the classical $\lambda/10{,}000$ requirement without any wavefront compensation. The next subsection explores this observation and explains it in terms of an outer working angle (OWA) limit due to our control scheme.

6.2. *Outer Working Angle Limit*

As shown in § 4.3, we chose to expand the λ-dependence of each spatial frequency in a Laurent-type expansion and to control the larger terms, that is, $\{f_{m,n}^0, f_{m,n}^{-1}, f_{m,n}^{-2}\}$, using a limited number of DMs. However, as shown in equations (38a)–(38f), this expansion is

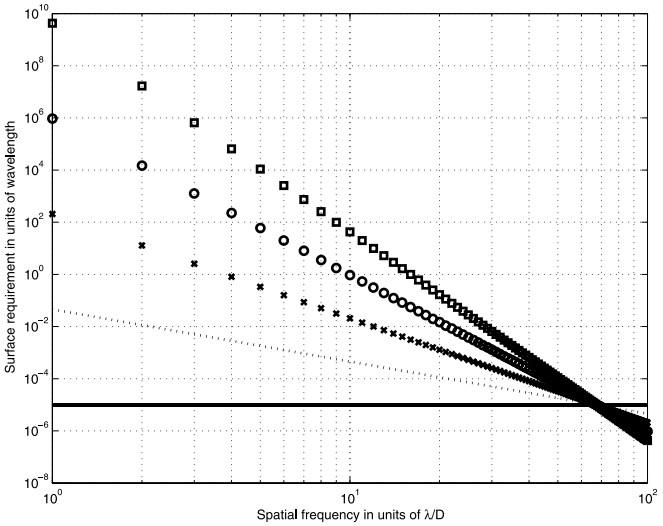

FIG. 9.— Surface requirements due to Fresnel propagation for a bandwidth of $\Delta\lambda/\lambda_0 = 0.1$. As a theoretical exercise, we assumed a control scheme that would correct up to order q in $\pi\lambda_0 z(n^2 + m^2)/D^2$: $\{f_{m,n}^{-1}, \ldots, f_{m,n}^{q}\}$. *Solid line*, requirement due to the zeroth-order phase errors $f_{m,n}^{-1}$; *dotted line*, requirement due to the first order, $f_{m,n}^{0}$; *crosses*, requirement due to the second order, $f_{m,n}^{1}$; *circles*, requirement due to the third order, $f_{m,n}^{2}$; *squares*, requirement due to the first order, $f_{m,n}^{3}$. We note that correcting higher orders relaxes the requirement for low spatial frequencies but increases the negative slope of the requirement in such a way that they all meet the zeroth-order requirement for a spatial frequency $N_{\rm limit}$.

carried out assuming that $\pi\lambda_0 z(n^2 + m^2)/D^2 \ll 1$. Clearly, this approximation breaks down for high spatial frequencies, and we would expect any control scheme based on this approximation to fail. In Figure 9, we show the surface requirements for a broadband null yielded by compensation with q DMs, even though we showed earlier that two would be sufficient for a planet-finding contrast. The resulting requirements converge for a specific spatial frequency that can be derived as follows in the case of two sequential DMs. In order to evaluate the phase requirements, we assume that the optics do not possess reflectivity errors. For two sequential DMs, equation (54) gives an expression for the polychromatic halo. By inspection of equations (38a)–(38f), the leading term of the λ-expansion of the $f_{m,n}^{-k}$ after correction is given by the $b_{m,n}$-dependent term:

$$I_{m,n}^{\rm 2DM} = \frac{1}{\Delta\lambda}\int_{\Delta\lambda}\left| i\frac{2\pi^2 b_{m,n}\lambda_0 z^2 (n^2+m^2)^2}{D^4}\lambda\left(1-\frac{\lambda_0^2}{\lambda^2}\right)\right|^2 d\lambda, \tag{60}$$

where we have assumed that the controllable $f_{m,n}^{-1,\rm 2DM}$ degree of freedom provided by the wavefront actuator perfectly compensates for the $f_{m,n}^{-1}$ term at $\lambda = \lambda_0$ and is the main source of the leakage otherwise. This halo is an increasing function of the spatial frequency. We define $n_{\rm limit}$ as the spatial frequency for which the surface requirement is the same with or without the wavefront actuator. Assuming a 10^{-10} target contrast, the surface requirement without any compensating optics is $b_{m,n} < 10^{-5}$; for an actuator with two sequential DMs, it is given by inverting equation (60). By equating these two requirements, we can solve for $N_{\rm limit} = (n_{\rm limit}^2 + m_{\rm limit}^2)^{1/2}$, which yields, after some algebra,

$$N_{\rm limit} = \frac{D}{\sqrt{\lambda_0 z}}\frac{3^{1/8}}{2^{1/8}(\Delta\lambda/\lambda_0)^{1/4}}. \tag{61}$$

Note that for $\Delta\lambda = 0$ this bound does not exist. Another upper bound in OWA, which has not been considered in this work, is the limit due to the finite number of actuators on the DM, which is roughly given by $N_{\rm actuators}/2$. Thus, for a 96×96 actuator DM, spatial frequencies above $48\lambda/D$ are uncontrollable. In contrast, if we assume a 1 cm pupil under a central wavelength of 1 μm, and with $\Delta\lambda/\lambda_0 = 0.4$, we see that a propagation of 1 m yields a Fresnel-induced OWA limit of $N_{\rm limit} = 10$, which is well below the actuator limit of 48. While this limit is not a showstopper, it does provide guidance in how fast a system needs to be to overcome the Fresnel limits and thus should be considered early in the optical design of such a coronagraph.

7. CONCLUSION

In this paper, we first presented an analytical treatment of Fresnel propagation in telescopes and derived a closed form for the propagated aberrated wavefronts. This methodology allowed us to bound the change in PSF structure due to Fresnel effects and to show that it can be lowered to the level of regular amplitude aberrations in the case of sufficiently oversized optics. We then delved into the polychromatic correction of propagated wavefront aberrations using a Fourier methodology. We first highlighted the dominant chromatic terms in the λ-expansion of the Fourier coefficients of the wavefront error. Then we presented a series of configurations using several DMs that take advantage of such a set of measurements in order to create a polychromatic null. Finally, we derived the surface requirements for each configuration and derived an outer working angle limit for these compensation schemes that is due to the high

coupling of amplitude and phase errors for high spatial frequencies. These concepts ought to be coupled with wavefront-sensing schemes based on wavelength diversity, which will be the topic of a future communication and tested in the Princeton *Terrestrial Planet Finder* laboratory. While our approach has been carried out in the case of a space telescope, it can been generalized to study the chromaticity of quasi-static speckles for ground-based high-Strehl systems and is thus useful for the understanding of extreme adaptive optics PSFs.

REFERENCES

Aime, C., Soummer, R., & Ferrari, A. 2002, A&A, 389, 334
Give'on, A. Kasdin, N. J., Vanderbei, R. J., & Avitzour, Y. 2006, J. Opt. Soc. Am. A, 23, 1063
Give'on, A., Kasdin, N. J., Vanderbei, R. J., Spergel, D. N., Littman, M. G., & Gurfil, P. 2003, Proc. SPIE, 5169, 288
Goodman, J. 1968, Introduction to Fourier Optics (San Francisco: McGraw-Hill)
Kasdin, N. J., Vanderbei, R. J., Spergel, D. N., & Littman, M. G. 2003, ApJ, 582, 1147
Littman, M. G., Carr, M., Leighton, J., Burke, E., Spergel, D. N., & Kasdin, N. J. 2003, Proc. SPIE, 4854, 405
Malbet, F., Yu, J. W., & Shao, M. 1995, PASP, 107, 386
Noecker, C., Woodruff, R. A., & Burrows, C. 2003, Proc. SPIE, 4860, 72
Pueyo, L., Littman, M. G., Kasdin, J., Vanderbei, R., Belikov, R., & Give'on, A. 2005, Proc. SPIE, 5903, 190
Shaklan, S. B., & Green, J. J. 2006, Appl. Opt., 45, 5143
Spergel, D., & Kasdin, J. 2001, BAAS, 33, 1431
Trauger, J. T., & Traub, W. A. 2007, Nature, 446, 771